Appendix A

THE LDCM ACTUATOR FOR VIBRATION SUPPRESSION *

Eric N. Ide and Douglas K. Lindner

Bradley Department of Electrical Engineering
Virginia Polytechnic Institute
Blacksburg, Va. 24061

ABSTRACT

A linear DC motor (LDCM) has been proposed as an actuator for the COFS I Mast and the COFS program ground test Mini-Mast. The basic principals of operation of the LDCM as an actuator for vibration suppression in large flexible structures are reviewed. Because of force and stroke limitations, control loops are required to stabilize the actuator, which results in a non-standard actuator-plant configuration. A simulation model that includes LDCM actuator control loops and a finite element model of the Mast is described, with simulation results showing the excitation capability of the actuator.

1.0 INTRODUCTION

A linear DC motor (LDCM) has been proposed as an actuator on the COFS-I Mast and the COFS ground test article Mini-Mast. This actuator has physical limitations which impose limits on its ability to generate force. The configuration of the mast/actuator system gives rise to a non-standard plant/actuator configuration. Feeding back the digital relative position measurement causes impure force generation. This paper will focus on how these facts arise and how they affect the use of the LDCM actuator for vibration suppression in large flexible structures.

The paper will start with a description of the LDCM actuator in Section 2. This section will include a description of the force limitations of the actuator. Section 3 will describe the mast/actuator system including compensation of the actuator. Section 4 describes the simulations performed and presents results.

2.0 ACTUATOR DESCRIPTION

The actuator proposed for use in the COFS program is a linear DC motor (LDCM). The LDCM consists of two parts. The stationary base will mount on the mast. It contains the motor coils and drive circuitry. The reaction mass is the bar which moves on bearings through the base. The bar contains permanent magnets to generate the motor flux.

A force applied to the reaction mass via the motor coils will apply an equal and opposite force to the base and hence, the mast. Two sizes of actuators are being built. A Type I actuator has an 11.6 kilogram reaction mass and a 15 centimeter stroke. A Type II actuator has a 6.8 kilogram reaction mass and a 7 centimeter stroke.

The physical characteristics of the LDCM actuator place limits on the amount of force it can generate. The force generated by the reaction mass is governed by Newton's Law,

$$F = ma, \tag{1}$$

where a is the second derivative of the reaction mass inertial position. Looking at sinusoidal excitation and taking the maximum gives,

$$F_{max} = m d \omega^2, \tag{2}$$

where d is the stroke length of the excitation. Thus, at low frequencies, the maximum force available is limited by the stroke limit of the reaction mass. At high frequencies, the maximum force is limited by the power available to be delivered by the power electronics. Fig. 1 shows the maximum force output for the two types of actuators versus frequency.

3.0 SYSTEM DESCRIPTION

A model of the actuator mounted on the COFS Mast is formed to examine system performance. Fig. 2 shows a representation of the actuator mounted on the mast. The equations of motion of the reaction mass are:

$$m\ddot{x} = F_{LDCM} \tag{3}$$

where x = reaction mass inertial position. A finite element model of the mast gives the mast equations of motion as:

$$\ddot{q} + D\dot{q} + Kq = BF_{MAST} \tag{4}$$

$$P = Cq$$

* This work was supported in part under NASA Grant NAG-1-719.

where P = mast inertial position. The force on the reaction mass is equal and opposite to the force on the mast.

$$F_{LDCM} = - F_{MAST} \quad (5)$$

F_{LDCM} is directly related to the current input to the actuator. These equations of motion are represented in Fig. 3, a block diagram of the uncontrolled LDCM actuator and mast. In this configuration, the actuator is unstable. Hence, actuator stabilization loops are required.

Fig. 4 shows a possible concept for stabilization of the actuator. The configuration is essentially position-velocity feedback. The velocity of the reaction mass is obtained by integrating the output of an accelerometer mounted on the reaction mass. The only position measurement available is a digital measurement of the reaction mass relative position, the difference between the reaction mass inertial position and the mast inertial position. Feeding back the relative position places the mast in the feedback path. Thus, the actuator control loops couple the actuator to the mast in a feedback configuration rather than the usual cascade configuration.

Also, feeding back the digital relative position measurement has other effects. Each time the measurement device steps in quantization level, a spike will be generated in the LDCM force. These force spikes result in impure force being applied to the structure.

4.0 SIMULATIONS

Simulations were used to evaluate the performance of the system. We will examine the behavior of the COFS Mast with ten LDCM actuators mounted on it. Four Type I actuators will be located at the tip of the mast in a square configuration. This allows the tip actuators to apply force in either direction as well as torsionally. Six Type II actuators will be placed in orthogonal pairs along the length of the structure.

A finite element model was used for the mast. Sixteen modes, 6 rigid body and 10 flexible, were used in the model. All frequencies were below 7 Hz.

A model for each actuator was generated from the block diagram in Fig. 4. The model contains all nonlinearities such as force saturation, stroke limits, and digital position measurement for all ten actuators. A fourth-fifth order, variable step size Runge-Kutta differential equation solver was used in the simulations.

The system was excited by applying a sinusoidal relative position command to one actuator. The following figures show simulation results from an excitation frequency corresponding to the second bending mode in the x direction (f = 1.36 Hz). The actuator used for excitation was the one which would be most effective in exciting the mode being analyzed. All other actuators were given a zero command. After five cycles of excitation, all actuators were given a zero relative position command to allow the structure to free decay.

Fig. 5 shows the mast inertial position at the actuator location where excitation occurred. The mast model included a small amount of inherent damping. The simulations showed an increase in damping. Thus, the actuator stabilization loops changed the behavior of the plant due to its location in the feedback path.

Fig. 6 shows the force output of the same actuator. Notice that the actuator continues to generate force after the command signal has been turned off. This is due to the component of the mast position in the force.

Fig. 7 shows the power spectral density of the LDCM force output of the exciting actuator during the excitation phase. The force spiking due to the digital relative position measurement generates the noise level shown on the graph. This is an example of the impure force generated by the actuator.

5.0 CONCLUSIONS

This paper has outlined the use of the LDCM actuator for vibration damping on flexible structures. The stroke length and power electronics limit the maximum force generated by the actuator. The actuator must be stabilized because it is open loop unstable. The available measurements for feedback place the plant in the feedback path. Thus, the actuator stabilization loops affect the plant behavior. Selected simulations showed the excitation capability of the actuator and impure force characteristics.

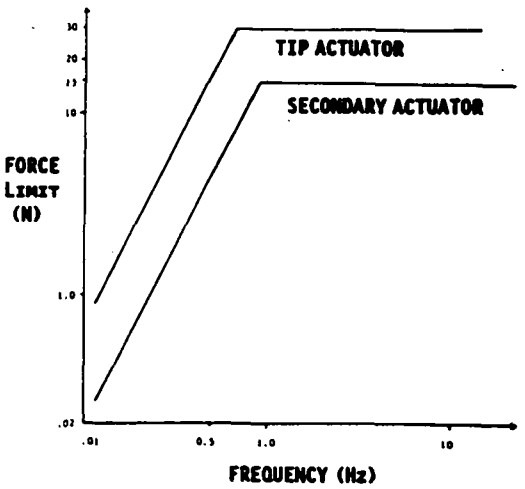

Fig. 1. Maximum Force Output

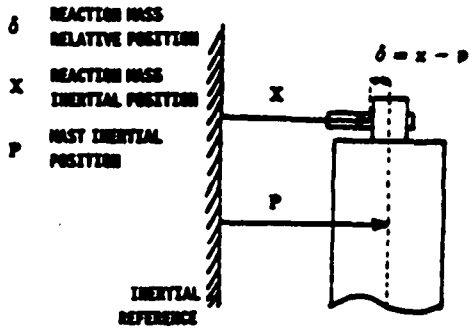

Fig. 2. Actuator Mounted on Mast

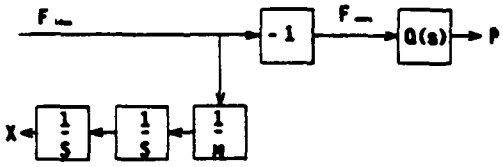

Fig. 3. Uncontrolled Actuator

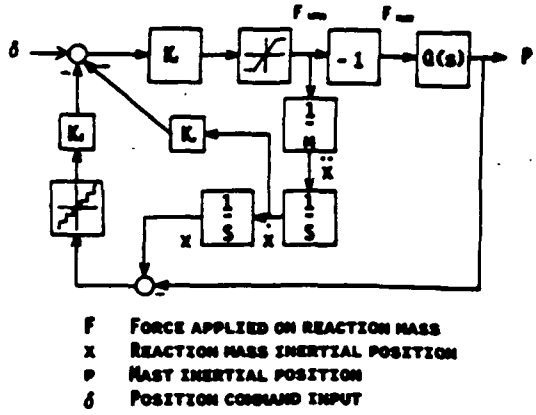

Fig. 4. Actuator Stabilization Loops

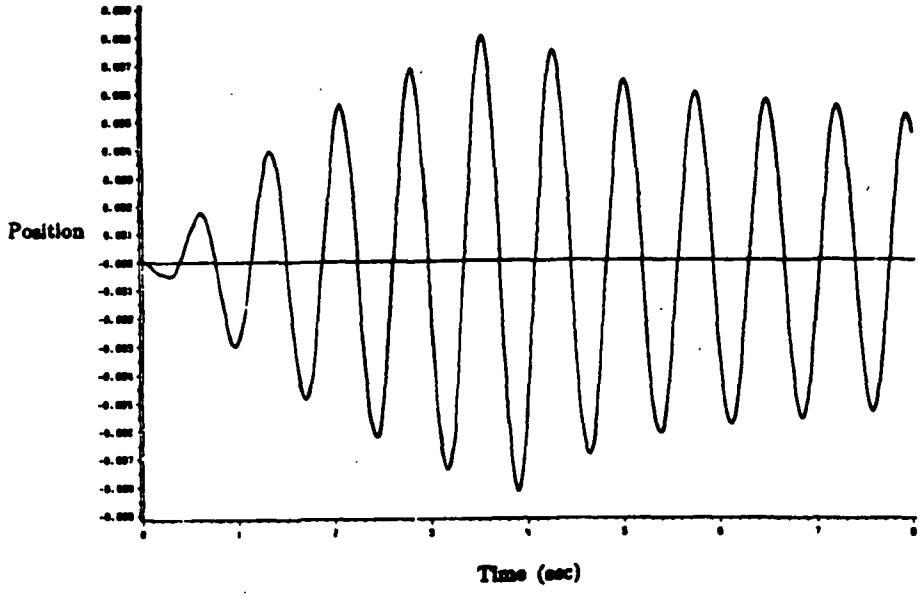

Fig. 5. Mast Inertial Position

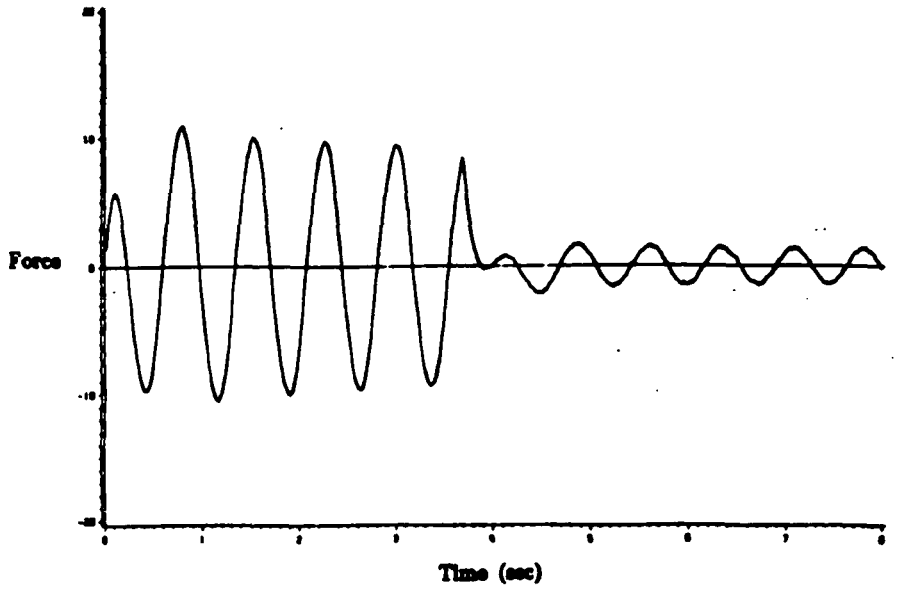

Fig. 6. Force Output of Exciting Actuator

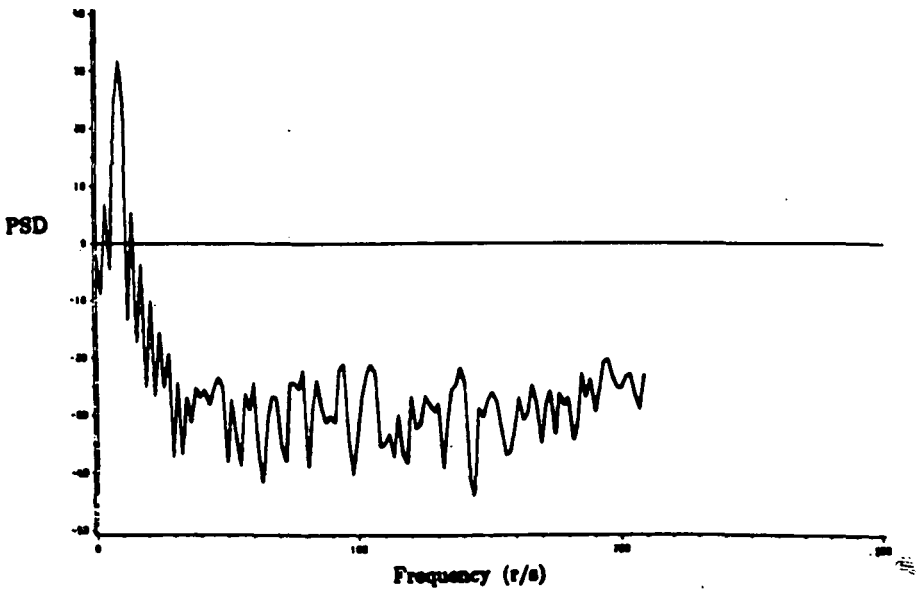

Fig. 7. Power Spectral Density of Force During Excitation